MULTI-OBJECTIVE OPTIMISATION TECHNIQUES FOR THE REDUCTION OF TORQUE RIPPLES IN SWITCHED RELUCTANCE MOTOR

Deepa Nidanakavi[a], Dr.Krishnaveni.K[b] and Dr Mallesham.G[c]
[a]Department of Electrical Engineering, Osmania University, Hyderabad, India,
deepanidanakavi@gmail.com.
[b]Department of Electrical and Electronics Engineering, CBIT, Hyderabad, India.
Krishnaveni_eee@cbit.ac.in.
[c]Department of Electrical Engineering, Osmania University, Hyderabad, India.
gm.eed.cs@gmail.com.

Abstract: Torque ripple is considered the effect that can be seen in most of the designs of electric motors, which refers to the periodic decrease or increase in the output torque when the motor shaft rotates. Torque ripple can be measured by the difference between the minimum and maximum torque on one complete revolution, and it can be expressed in percentage. Switched reluctance motor is a simple structure with strong fault tolerance and robustness that can be widely used in electrical and industrial fields. Due to the unique feature of switched reluctance motor, excessive torque ripple occurs in the magnetic circuit, which is considered the major limitation. Thus, the reluctance motor produces higher vibration and acoustic noise by introducing a high current ripple in the input side of the inverter. Torque Sharing Function and Direct Instantaneous Torque Control (DITC) is helpful in suppressing torque ripple. The research study proposes optimizing the hysteresis band according to torque error and torque ripple reduction. The proposed control model can be implemented by decreasing the inverter's size and increasing the volumetric power density.
Keywords: Torque Ripple, Optimization, Torque Ripple Reduction, Switched Reluctance Motor, TSF-DTIC

Introduction

Switched Reluctance motor has numerous advantages, including simple and rugged structure, robust fault tolerance, high reliability, high efficiency, high output, wide range, ample starting torque and applications in few conditions and high speed [1]. The main advantage is its suitability for driving a motor in an electric vehicle even though it has a few limitations, like torque ripple of SRM leads to the uneven running of a motor rotor that results in noise and vibration that may affect the comfort and stability of electric vehicles. Additionally, the motor's dynamic performance is more significant for traction characteristics in electric vehicles. SRM is referred to as the electromechanical conversion device with non-linear characteristics and salient pole structure. The non-linear relationship of torque and flux with the position angle of the rotor and phase current may lead to torque ripple in the larger motor, which directly affects the output dynamic characteristics of the SRM system. The optimization design and torque

reduction of SRM are mostly discussed nowadays. The main characteristics and scheme focused on the optimization parameters of motor design and control strategies. The process of torque ripple reduction and noise reduction can be used in the framework of the SRM rotor pole [2].

More torque ripple is caused due to tracking errors among reference torque and actual torque in the "Direct Instantaneous Torque Control" algorithm present in the commutation region of SRM depending upon the "Torque Sharing Function". The compensation method of torque combines TSF-DITC with the simulation control method is proposed. The sectors are subdivided into commutation regions by considering the position of the rotor. Various types of voltage states are selected in various sectors for the complete compensation of tracking the errors between the reference torque and the actual phase torque distributed by the TSF by reduction of torque ripple. Similarly, the DITC algorithm effectively reduces the candidate voltage state at the current time by reducing the computational burden—the performance comparison of simulation with the TSF-DITC algorithm for dynamic performance and steady-state [3].

The Switched Reluctance Drives are due for electrification in many products in industries that includes hybrid or electric vehicles, healthcare, white-goods, and electric aircraft in Switched Reluctance Machine for the potential prospect satisfaction of ability of operation, low-cost, fault-tolerance, harsh environment, robust structure over the wide range of speed. The research focuses on the torque control of SRD with the achievement of implementation cost, weight, smaller size, robustness, high reliability, minimal torque ripple and zero torque error. "Direct Instantaneous Torque Control and Direct Torque Control "are the standard method for obtaining desired torque characteristics, including minimised torque ripple and optimal torque density, even though the torque control methods are compared to the conventional hysteresis control model, which requires using of power devices of about 150% for the achievement of desired superior performance—the requirement of stress, conduction loss and extra cost on the machine winding and semiconductors of the drive. The intuitive and straightforward method of torque controlling depends upon adaptive control. The torque control approach is designed to consider control techniques for SRD based on the complexity of information flow [4].The switched reluctance motor's high torque ripples, brought on by the doubly salient structure, restrict its industrial application. In order to lessen the torque ripple of SRM with 4 phases with improved direct torque control for the observer and controller of sliding mode is developed in the research study. In order to design the sliding mode speed controller for the DTC system new reaching law was first developed for the sliding mode controller. The SMSC is combined with an "Anti-Disturbance Sliding Mode Observer" to create the composite of anti-disturbance speed control strategies. The validation of in-depth simulation is performed to demonstrate the efficacy of ADSMO, SMSC and new reaching law. The proposed model's performance ADSMO-SMSC is evaluated with a DTC system comprised of 4 phase prototype SRM is finally tested [5].

Reliability is a major concern in industries where Switched Reluctance Motors (SRM) are becoming more prevalent, such as automotive, aerospace, and home appliances. Consequently, it is essential to guarantee the hardware and control algorithm for the motor drive. This work uses theoretical and simulation analysis to characterise the complexity and reliability of several popular control approaches for SRM drives. The impact of typical SRM drive errors on the

dependability of its control systems is examined. In addition, an analysis of the relationship between information flow complexity within the control approach and the reliability of SRM control is offered. Three techniques are taken into consideration and contrasted: “Torque Sharing Function-based Direct Instantaneous Torque Control, Direct Torque Control (DTC), and Current Chopping Control (CCC)”. According to the data, the TSF-DITC approach is the most resilient to measurement error, followed by the DTC and CCC. The TSF-DITC approach maintained excellent resilience and dependability but produced superior torque characteristics [6].

Two unique approaches are put forth to reduce torque ripple for switched reluctance motors (SRM). It combines direct instantaneous torque control and torque sharing function to integrate TSF with model predictive control. In order to compare the two methods, their control block diagrams are first introduced in depth along with their fundamental ideas. Second, the simulation in MATLAB/Simulink is used to validate the proposed two control systems. Eventually, the simulation results demonstrate that the two strategies correctly reduce torque ripple. Also, the two algorithms' steady and dynamic state performances are contrasted in this work. According to the study, the TSF+MPC scheme can offer minor torque ripple reduction and higher controlled performance [7].Electric motors are used in various applications, and their essential requirements include an increased specific power, decreased cost, and dynamic construction. Switching reluctance is one such motor that meets all the requirements listed above. Switching reluctance machines are a growing rival to traditional induction and permanent magnet motors in small, commercial, and electric vehicle (EV) applications. The main drawback of SRM is torque ripple, particularly during the operation at high speed, which results in acoustic noise even though SRMS offers significant advantages over permanent magnet and induction motors. The systems may sometimes suffer from these drawbacks, which depend upon the application which is to be used for acoustic noise and torque ripple form can be harmful. This article examines the state of technology and current developments in switching reluctance machines that minimize torque ripples [8].

The problem of the research study is the multi-objective optimisation of Torque ripple reduction of TSF-DITC controlled switched reluctance motor. The objectives of the research study are using three optimization techniques for torque ripple reduction of TSF-DITC controlled Switched Reluctance Motor such as grasshopper optimisation, Game theory optimisation, Hybrid Sin-Cosine and Spotted Hyena Optimizer based Chimp Optimization. Further section II explains about SRM Drive System, section III Conventional Methods, and section IV Improved Method, section V explains about Optimization Techniques, section VI simulation results and Validation.

Mathematical Model of SRM Drive System

Basic Equations of Torque Ripple Reduction

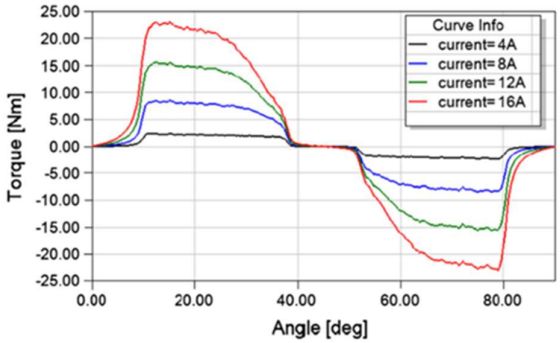

Figure 2.1: Finite Element Analysis Static Torque Characteristics of 6/4 SRM

$$V = iR + \frac{d\lambda}{dt} \tag{2.1}$$

Where λ is the function of I and θ

$$\frac{d\lambda}{dt} = \frac{d}{dt} i + \frac{di}{dt}\theta$$

$$V = iR + \frac{d(L\lambda)}{dt}$$

$$V = iR + L\frac{di}{dt} + i\omega\frac{dL}{d\theta}$$

$$V = iR + L\frac{di}{dt} + i\frac{dL}{d\theta} x \frac{d}{dt}$$

$$V = iR + L\frac{di}{dt} + i\omega\frac{dL}{d\theta} \tag{2.2}$$

Where iR is the Ohmic drop

$L\frac{di}{dt}$ is the EMF caused by incremental inductance

$i\omega\frac{dL}{d\theta}$ is the self-induced EMF

$$V = iR + L\frac{di}{dt} + e \tag{2.3}$$

E is proportional to the current speed in Self-Induced EMF and the rate of inductance change with the rotor angle.

If the flat-topped current is assumed as $L\frac{di}{dt} = 0$, on the other hand, inductance is considered to be constant as self EMF is 0. So, the first term $L\frac{di}{dt}$ absorb all the applied Voltage

$$V_i = i^2R + L\frac{di}{dt} + i^2\omega^2\frac{dL}{d\theta} \tag{2.4}$$

Energy stored in magnetic circuit $= \frac{1}{2} = Li^2$

Rate of change of Stored energy in magnetic circuit $= \frac{d\theta}{dt}\left[\frac{1}{2}Li^2\right]$

$$= \frac{1}{2} L.2i \frac{di}{dt} + \frac{1}{2} i^2 \frac{dL}{dt}$$

$$= Li \frac{di}{dt} + \frac{1}{2} i^2 \frac{dL}{d\theta} x \frac{d\theta}{dt}$$

$$\frac{dW_{mag}}{dt} = Li \frac{di}{dt} \frac{1}{2} i^2 \omega \frac{dL}{d\theta} \quad (2.5)$$

Transferred Mechanical Energy = Electrical energy input – rate of change of energy stored

$$= i^2 R + Li \frac{di}{dt} + \frac{1}{2} i^2 \omega \frac{dL}{d\theta} - i^2 R \frac{di}{dt} - \frac{i^2}{2} (\omega) \frac{dL}{d\theta}$$

$$P_m = \frac{1}{2} \left| i^2 \omega \frac{dL}{d\theta} \right| \quad (2.6)$$

In general,

$$P_m = \frac{2\pi NT}{60} = \left| \frac{2\pi N}{60} \right| T = \omega T$$

$$P_m = \omega T \quad (2.7)$$

From 3.7;

$$T = \frac{P_m}{\omega} \quad (2.8)$$

Substituting (2.6) in (2.8),

$$T = \frac{1}{2} \frac{\left| i^2 \omega \frac{dL}{d\theta} \right|}{\omega}$$

$$T = \frac{1}{2} \left| i^2 \frac{dL}{d\theta} \right| \quad (2.9)$$

Conventional Method to Reduce Torque Ripple

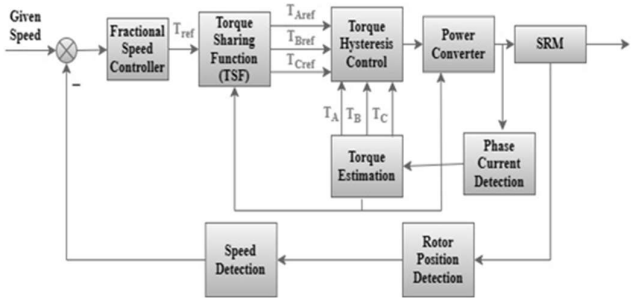

Figure 3.1 Fractional Order – DITC block diagram [2]

One of the existing conventional methods followed is Fractional Order-DITC method of SRM. The fractional speed controller output is the required synthetic reference torque of SRM.Expected torque based on present rotor position angleTSF can be used to obtain (TAref, TBref and TCref) as shown if figure 3.1. The torque hysteresis control is then utilised to ensure that each phase torque tracks the expected torque while minimising torque ripple. Based on the rotor angle and phase current data, the interpolation lookup table Te (θ, i) generates the torque

feedback signal for each phase.

Proposed Improved Method - Mathematical Model of Torque Ripple Reduction using the current control method

SRM equivalent circuit shown in figure 4.1.

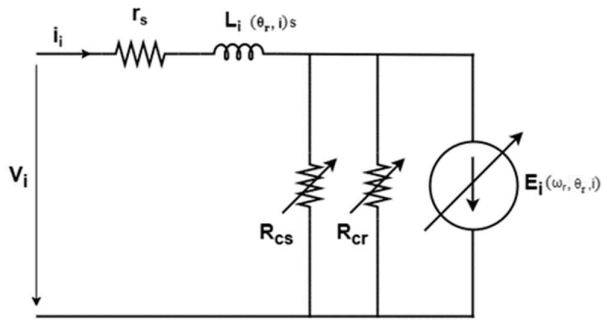

Figure 4.1 SRM equivalent circuit for Torque Ripple Reduction using the current control method

$$V_i = r_s i_i + L_t(\theta_r i)\frac{di_t}{dt} + E_i(\omega_r, \theta_r, i_i) \qquad (4.0)$$

Torque can be measured

$$T_e = \sum_{i=1}^{m} \frac{1}{2} i_i^2 \frac{\partial \lambda_i(\theta_r)}{\partial \theta_r}$$

(4.1)

T_{he} – Torque
i – Current
λ – flux
m- No.of.Poles
θ – Phase angle rotor

$$\theta_{\omega max} = \theta_m \frac{\pi}{Nr}$$

(4.2)

Measured θ

The angle position converted radiant to degree conversion

$$\theta_d = \theta * \frac{180}{TL}$$

(4.3)

The rotor angle updating,

$$\theta_r \begin{cases} \theta_r\theta_r = [0 \ -30 \ -60] \ \ for\ initial\ state \\ \theta_r\theta_r = Modulus\ of\ |\theta_r|, 90 \end{cases} \qquad (4.4)$$

$$\theta_{r1} = |\theta_r| \geq 45$$
$$\theta_{r2} = |\theta_r| \geq 75$$

Θ_{r1}, Θ_{r2} are the logical or Boolean outputs

Result updating

$$i_{result} = i_r * (\theta_{r1} * \theta_{r2})$$

(4.5)

i_r – Rated Current Value

$$i_{Err} = i_{result} - i_{actual} \quad (4.6)$$

i_{actual} - Measured current of SRM

i_{Err} – error current

Hysteresis Band

H_{limits}

H_{LL} – Hysteresis Lower Limit

H_{UL} – Hysteresis Upper Limit

$$i_{Err} > H_{UP} - ON$$
$$i_{Err} < H_{LL} - OFF$$

$H_{UP} > i_{Err} > H_{LL}$ - Remain same output, Output does not change

The voltage of DC to 3-Phase AC inverter

$$V_{ao} = \frac{2V_{DC}}{\pi}[cos\omega t - \frac{1}{3}cos3\omega t + \frac{1}{5}cos5\omega t - \cdots..]$$

(4.7)

$$V_{bo} = \frac{2V_{DC}}{\pi}[\cos\left(\omega t - \frac{2\pi}{3}\right) - \frac{1}{3}\cos3\left(\omega t - \frac{2\pi}{3}\right) + \frac{1}{5}\cos5\left(\omega t - \frac{2\pi}{3}\right) - \cdots..]$$

(4.8)

$$V_{co} = \frac{2V_{DC}}{\pi}[\cos\left(\omega t + \frac{2\pi}{3}\right) - \frac{1}{3}\cos3\left(\omega t + \frac{2\pi}{3}\right) + \frac{1}{5}\cos5\left(\omega t + \frac{2\pi}{3}\right) - \cdots..]$$

(4.9)

Phase to Phase Voltage

$$V_{ab} = V_{an} - V_{bn} = \frac{2\sqrt{3}V_{DC}}{\pi}[\cos\left(\omega t + \frac{\pi}{6}\right) + \theta - \frac{1}{5}\cos5\left(\omega t + \frac{\pi}{6}\right) - \frac{1}{7}\cos7\left(\omega t + \frac{\pi}{6}\right) + \cdots..]$$

(4.10)

$$V_{bc} = V_{bn} - V_{cn} = \frac{2\sqrt{3}V_{DC}}{\pi}[\cos\left(\omega t - \frac{\pi}{2}\right) + \theta - \frac{1}{5}\cos5\left(\omega t - \frac{\pi}{2}\right) - \frac{1}{7}\cos7\left(\omega t - \frac{\pi}{2}\right) + \cdots..]$$

(4.11)

$$V_{ca} = V_{cn} - V_{an}$$
$$= \frac{2\sqrt{3}V_{DC}}{\pi}[\cos\left(\omega t + \frac{5\pi}{6}\right) + \theta - \frac{1}{5}\cos5\left(\omega t + \frac{5\pi}{6}\right) - \frac{1}{7}\cos7\left(\omega t + \frac{\pi 5}{6}\right) + \cdots..]$$

(4.12)

Leading Phase-Shift of $\pi/6$

Vα i

V is directly proportional to i.

$$T_e = \sum_i^m \frac{1}{2} i_i^2 \frac{\partial \lambda_i(\theta_r)}{\partial \theta_r} \quad (4.13)$$

Here, the current is controlled by controlling voltage.

Optimization Techniques

The proposed methodology comprised a grasshopper optimisation algorithm, game theory optimisation, and Hybrid SSC Optimization Algorithm for torque ripple reduction and DC ripple reduction of TSF-DITC controlled Switched Reluctance Motor in figure 5.1. It consists of a current measurement for calculating the reference current with the actual current for finding the difference of minimized torque. The proposed methodology consists of a hysteresis band with a feedback signal above the band, and the plant can be operated in one state. When it is below the band, it operates in another state. If the feedback signal is within the hysteresis band, the state of operation is never changed. It consists of the torque converter, a fluid coupling that transfers the rotating power from the prime mover for converting into the rotating driven load. The converter is connected to the power source to the load in the automatic transmission of SRM. It constitutes SRM, the electric motor which it runs by the reluctance torque. It uses a mechanical commutator to switch the winding current like traditional motors.

The position of the electronic sensor is used to determine the Rotor shaft angle and the electronics in a solid state for switching the windings to enable dynamic control and pulse training.

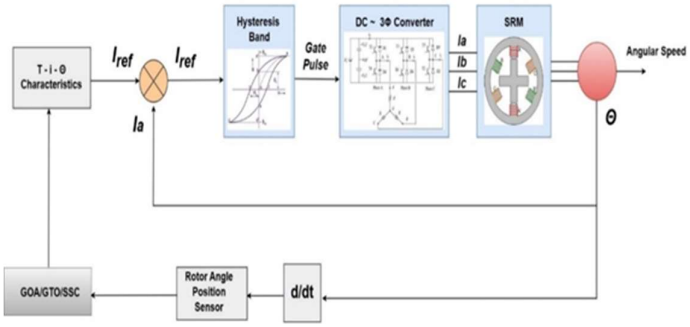

Figure 5.1 Proposed control system block diagram

5.1 Grasshopper Optimization Algorithm

The grasshopper optimisation algorithm is the population-based Meta heuristic algorithm. The recent swarm intelligence algorithm was introduced for solving the numerical optimisation issues. The inspiration of GOA Comes from the interaction and behaviour of grasshopper swarms in nature.

The central concept behind the GOA algorithm as the grasshopper swarm makes long-range moves and sudden jumps in the adulthood phase as they have wings—the swarm search for food by splitting into two stages of the process. The swarm search for a food source in the exploration phase, and the value positions are updated and computing fitness value. The best solution is found among all the available sources. Thus, the GOA algorithm mimics

grasshoppers' hunting method and social behaviour [10].

Game Theory Optimisation Algorithm

Game theory optimisation includes computing Nash Equilibrium using the Lemke-Howson algorithm. The algorithm uses the iterated pivoting using the simplex algorithm used in linear programming. The Nash equilibrium can be located using the Lemke-Howson algorithm using the Tableau method, a pivoting procedure. Pre-processing is the first step; the objective is restricting the game's options by iterating to maintain the dominant strategies [11]. As a result, the effort necessary to solve the problem is reduced in complexity. Each player in the game needs their own. With a constructed tableau in hand, we can now start pivoting. The entry and exit variables are the primary consideration here. Until the complementarity requirements are satisfied, the exit variable serves as the entry variable for the next pivot.

The algorithm flow is divided into four main steps. The first step, pre-processing, entails narrowing the solution space by excluding strictly dominated strategies. Tableaux Initiations entail building a tableau for each player in the game. The next step after creating all tableaux is pivoting. Multiple iterations of pivoting can be done to fund the output, which is the process's last step, by choosing the basis variable to enter and exit on.

SSC Optimization

The recently developed metal heuristic approach is the Chimp optimisation algorithm which is introduced from the inspiration of individual intelligence as well as the sexual motivation of the Chimps—the algorithm specially designed for trapping of local Optima for alleviation of slow conversion speed. The hybrid algorithm was developed based on the sign and cosine function and attacking strategies of the Spotted Hyena Optimiser. The hybrid optimisation is referred to as the "Sine Cosine and Spotted Hyena-Based Chimp Optimization Algorithm, " known as the SSC algorithm [12]. The algorithm helps find the best optimal solution to complex real-life problems. The attacking strategy of the SHO and Sine-Cosine algorithms helps in better exploitation and exploration. The strategy can be applied to updating the chimps' equation while searching to overcome the chimp optimisation algorithm's drawbacks, including local minima and slow convergence.

Hysteresis band

The relay block output switches among the two specific values of the hysteresis band as shown in figure 5.2. If the relay is on, then it remains until the drop of input shows below the value parameter of the switch-off point. If the relay point is off, it remains until the input exceeds the parameter's value in the switch-on point. The output is generated by accepting one block as input.

Converter:

DC to 3-phase converters to supply the power to SRM

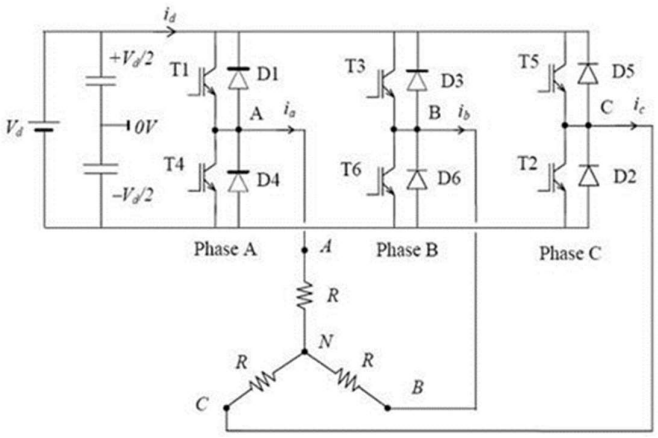

Figure 5.2 Block Diagram of TSF-DITC

Switched Reluctance Motor

The Switched Reluctance Motor concept dates back to the 1830s when numerous builders and inventors initially attempted to create the practical machine. Robert Davidson was one of them, and he created a reluctance motor to operate an electric locomotive in 1838. Early attempts had weak electromagnetic and mechanical designs and insufficient mechanical switches. The SRM had to wait 150 years for the theoretical underpinnings and new power electronics technologies to be introduced. In 1980, the fundamentals of a family of switching reluctance motors were established. The development of powerful microcontrollers and power electronics required an additional thirty years. Numerous businesses are making SRM worldwide right now, and over the next five years, the market is anticipated to expand by around 5.2%. SRM's construction can be modified to fit a variety of use cases [13].

Salient poles are present on the stator and the rotor in a typical SRM configuration. The stator has windings, and phase electric current flows in a single direction. The torque reluctance produces a rotary movement caused due to variation in the inductance function of the angle. The benefits of this straightforward design include low cost, dependability, excellent efficiency, and broad speed. Every energised winding of phase produces torque for the specific interval of rotor angle.

Thus, to activate and deactivate the phase current at the selected angle, SRM control strongly relies on information about the rotor position. The main flaw in SRMs is torque ripples that happen whileswitching off from one winding to another winding. The main objective of the research study is torque ripple reduction and to increase efficiency by optimising the motor's structure and magnetic design and utilising improved motor control.

A summary of SRM control methods is provided. Intelligence Control, Iterative Learning Control, Feedback Linearization Control, TSF-Based Control, Direct Torque Control, Average Torque Control, and Angle and Current Modulation are the different categorised techniques.

5.6 Parameters of SRM

The control methods are optimised and tailored for commercially available SRM. It consists of small 200 watts 3-phase 6/4 pole of SRM. The estimated voltage is 240 watts. Stator phase winding consists of 4 coils connected with the parallel series. The width of the rotor pole and stator pole is of the same size of about 6/4.However, the inductance profile has a sharp peak in

the aligned position, and the motor transition into generator mode is speed. The voltage may vary from 120V to 240 V. Few parameters considered for the SRM motor are discussed in Table 5.1.

Table 5.1 Parameters of SRM – 6/4 Motor specification

Number of rotor poles	4
Number of stator poles	6
Number of turns per pole	590
Stator pole arc	32°
Rotor pole arc	30°
Air gap length	0.5mm
Stator outer diameter	116mm
Stator length	48mm
Stator pole height	105mm
Rotor pole height	21mm
Shaft diameter	19mm
Unaligned inductance	48mH

5.7 Proposed system framework

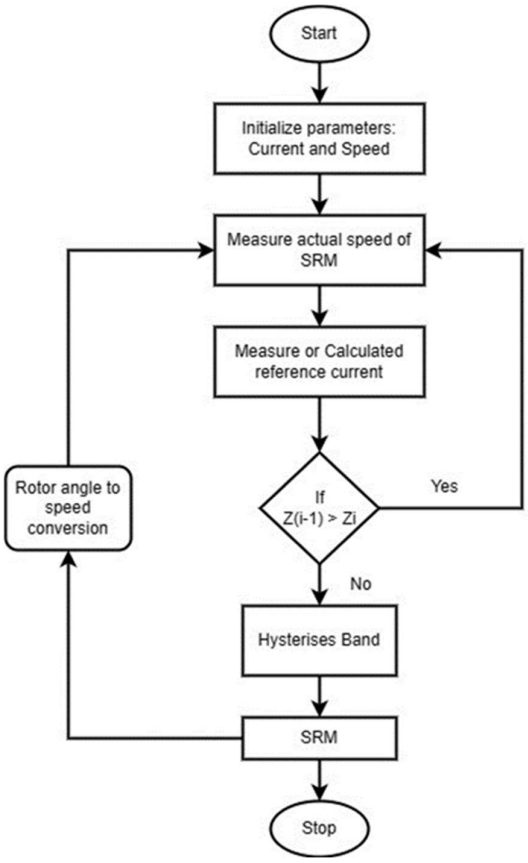

Figure 5.3 Flowchart of the proposed system

The proposed framework includes the following steps as given below;

Step 1: Start

Step 2: Initialisation of parameters current and speed

Step 3: Measurement of the actual speed of SRM

Step 4: Measurement and calculation of reference current

Step 5: If Z(i-1) > Zi
Step 6: If it is not, it goes with the Hysteresis band
Step 7: Then it moves to SRM
Step 8: If it is yes, rotor angle to speed conversion
Step 9: Stop
Where Z is current Error value.

Optimisation of the proposed Model

The proposed framework of optimisation includes the following steps as given below;
Step 1: Start
Step 2: Calculation of rotors angle using a grasshopper optimisation algorithm, Game theory optimisation and Hybrid Sin-cosine and SSC algorithm
Step 3: Gate pulse generation
Step 4: Inverter PC to 3
Step 5: SRM

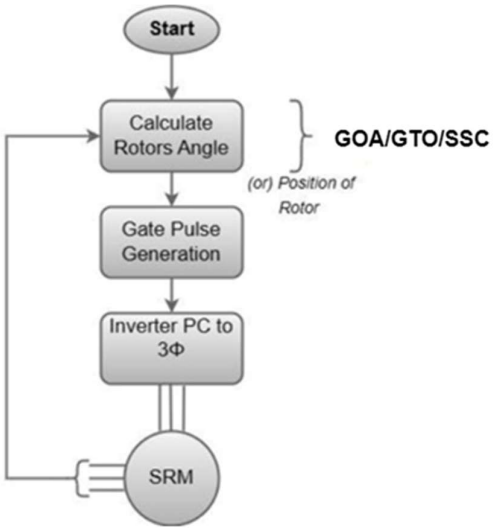

Figure 5.4 Optimisation used in the Flowchart of the system

Simulation Results – Discussion

The System simulation model comprised of 6/4 SRM motor built for the verification of the effectiveness and correctness of the proposed optimisation model in the MATLAB simulation environment.

6.1 System Simulation Model

The system simulation model consists of an optimisation algorithm for torque ripple reduction in SRM with a specific mode of 6/4. It consists of a hysteresis band converter and a power of 240 volts. TSF-DITC is considered the primary method for suppressing the torque ripple. The method uses the TSF for the distribution of total torque in the individual phase, whereas for controlling the appropriate torque-hysteresis-driven motor rules. The multi-objective converter in the SRM selects the corresponding rules on the conduction region for accelerating the demagnetisation and excitation in the region of commutation and achieving fast torque tracking. DITC algorithm for SRM based on the optimal angle adaptive TSF included in the

Simulation model. The TSF of dynamic and shapeless nature is used to improve system efficiency in torque ripple reduction of SRM. Different types of commutation points have a great influence. Since the optimisation algorithm is simple and easy to implement for torque reduction of SRM, torque ripple reduction is required to form complex hysteresis control rules in the region of commutation. The multiple objective optimisations of GOA, GTO and SSC algorithm helps overcome the difficulties of optimising multiple performances simultaneously.

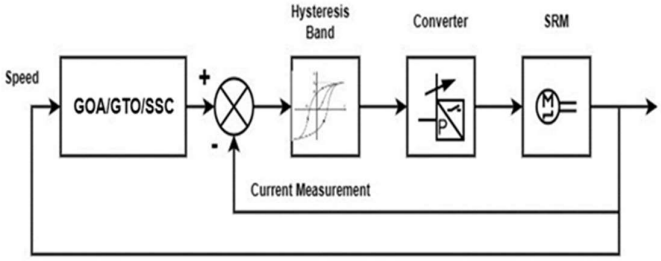

Figure 6.1 Proposed System Model

6.2 Hysteresis Band Output

After the system simulation model predictive control method, the effectiveness assessment is carried out in TSF-DITC. The rate of current change, the power converter capability, and other factors or considered [14]. The band output is calculated for three optimisations of the hysteresis band according to time. The comparison of simulation and experimental results are displayed in Figure 6.2. The proposed hysteresis banned output compares the torque ripples and tracing ability. The hysteresis band and overlapping angle influence the torque ripple. The current and other hysteresis band is set from 0.1 A to 1 A.

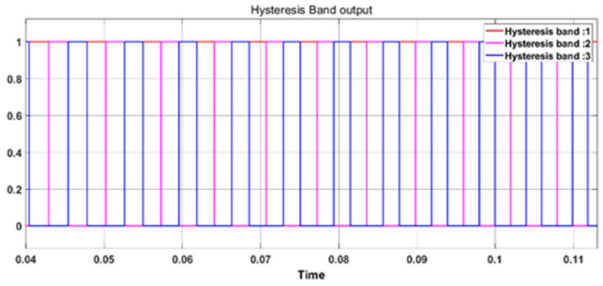

Figure 6.2 Hysteresis Band Output

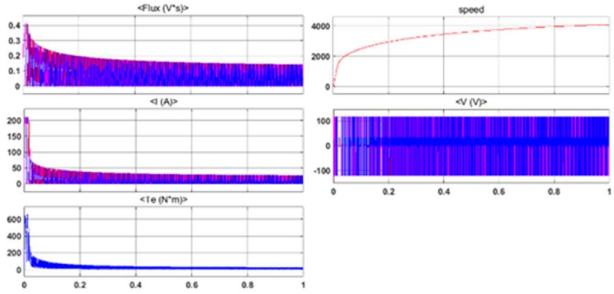

Figure 6.3 Simulated flux linkage, current and torque, speed, and voltage waveforms corresponding to three phases of the investigated 6/4 SRM

The current and simulated flux linkage and torque are proportional to each other, and they may vary similarly concerning the axis of time. Initially, the current and torque are very high. The

relationship between inductance and speed while tracking the reference speed according to the actual speed with the moment of inductance remains constant. It remains constant and gets settled down. Concerning the actual speed, their reference speed is tracked quickly in comparison to 4-phase switched reluctance. The actual speed is 0.04 seconds. Initially, the current is very high because the inrush current lies within 5 A. If dL/dθ is positive, torque is also positive, and if the value is negative, Torque is also harmful.

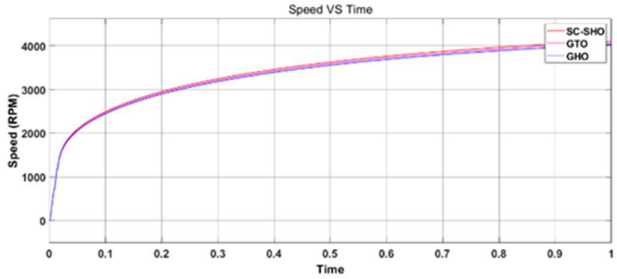

Figure 6.4 Comparative performance of GOA, GTO, SC-SHO optimisation for Speed

The comparative performance of 3 optimisation algorithms like grasshopper optimisation algorithm, game theory optimisation hybrid algorithm of sine cosine and spotted hyena optimiser for calculation of speed versus time. The graph in Figure 6.4 shows that the SC-SHO algorithm produces more speed for SRM.

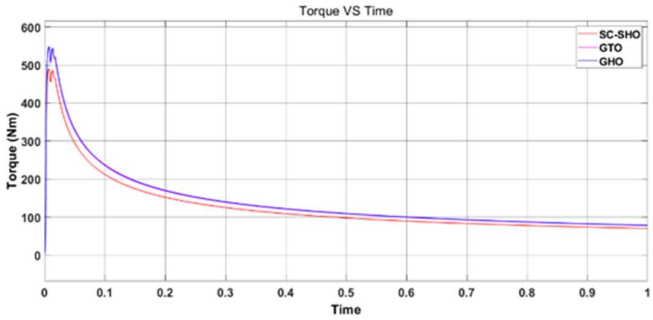

Figure 6.5 Comparative performance of GOA, GTO, SC-SHO optimisation for Torque Ripple Reduction

The comparative performance of 3 optimisation algorithms, grasshopper optimisation algorithm, game theory optimisation, the hybrid algorithm of sine cosine and spotted hyena optimiser for torque ripple versus time calculation. The graph displayed in Figure 6.5 shows that the SC-SHO algorithm is better in torque ripple reduction for and DC Ripple reduction of TSF-DITC controlled Switched Reluctance Motor.

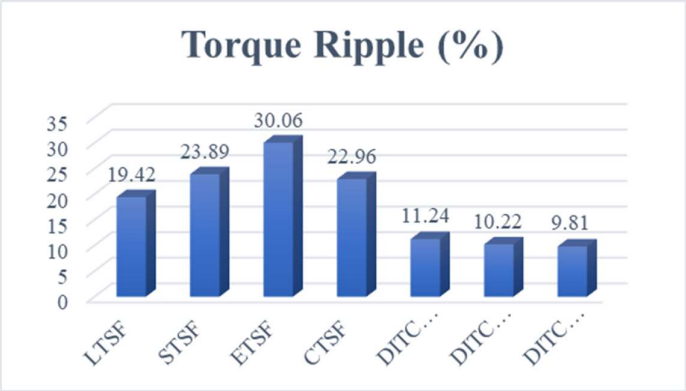

Figure 6.6 Torque ripple reduction validation of proposed optimisation

The proposed optimisation techniques have been validated with existing approaches regarding torque ripple reduction, as shown in Figure 6.6. It is visible that the proposed GOA, GTO, and SSC has torque ripple reduction percentage of 11.24, 10.22, and 9.81 of 6/4 pole SRM Motor, respectively. The obtained results proved that torque ripple reduced in the proposed system compared to existing Linear TSF, Sinusoidal TSF, Exponential TSF, and Cubic TSF of 19.42, 23.89, respectively 30.06, 22.96 of 8/6 pole SRM Motor [15]. Regarding speed and time characteristics, the proposed method achieved earlier stabilization [16], as shown in Figure 6.7.

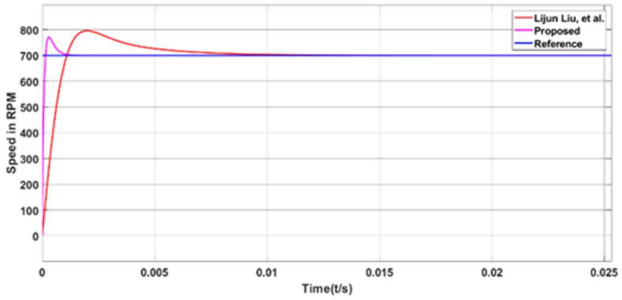

Figure 6.7 Speed Vs Time Validation of proposed optimisation

7. Conclusion

To conclude this research study, the grasshopper optimisation algorithm and game theory optimisation algorithm is used for Torque ripple reduction of TSF-DITC controlled Switched Reluctance Motor. Hybrid Sin-cosine and Spotted Hyena Optimizer-based Chimp Optimization Algorithm are used for Torque ripple reduction and DC Ripple reduction of TSF-DITC controlled Switched Reluctance Motor. According to the simulation results of hysteresis band output and the comparative performance graph, it is shown that the SC-SHO optimisation algorithm shows better results in torque ripple reduction than GOA and GTO comparatively. The future scope of the study is to develop simple and efficient algorithms for fault-tolerance and fault-diagnosis techniques.

References

Honghua, W. (1995). Speed control technology of switched reluctance motor [M].

Liu, L., Zhao, M., Yuan, X., &Ruan, Y. (2019). Direct instantaneous torque control system for switched reluctance motor in electric vehicles. The Journal of Engineering, 2019(16), 1847-1852.

Yang, Y., Xu, A., Leng, B., Sun, J., & Li, K. (2022). Torque Compensation Method of Switched Reluctance Motor Adopting MPC Based on TSF-DITC. Progress In Electromagnetics Research M, 110, 211-221.

Dankadai, N. K. (2022). Multi-objective torque control of switched reluctance machine (Doctoral dissertation, Newcastle University).

Sun, X., Wu, J., Lei, G., Guo, Y., & Zhu, J. (2020). Torque ripple reduction of SRM drive using improved direct torque control with sliding mode controller and observer. IEEE Transactions on Industrial Electronics, 68(10), 9334-9345.

Dankadai, N. K., Elgendy, M. A., McDonald, S. P., Atkinson, D. J., & Atkinson, G. (2019, October). Investigation of reliability and complexity of torque control for switched reluctance drives. In 2019 IEEE Conference on Power Electronics and Renewable Energy (CPERE) (pp. 485-490). IEEE.

Ren, P., Zhu, J., Guo, Z., Song, X., Jing, Z., & Xu, A. (2021, May). Comparison of Different Strategies to Minimise Torque Ripples for Switched Reluctance Motor. In 2021 IEEE 4th International Electrical and Energy Conference (CIEEC) (pp. 1-6). IEEE.

Deepa, N., Krishnaveni, K., &Mallesham, G. (2022). Recent Trends in Minimization of Torque Ripples in Switched Reluctance Machine.

Ye, J., Bilgin, B., & Emadi, A. (2014). Elimination of mutual flux effect on rotor position estimation of switched reluctance motor drives. IEEE Transactions on Power Electronics, 30(3), 1499-1512.

Meraihi, Y., Gabis, A. B., Mirjalili, S., &Ramdane-Cherif, A. (2021). Grasshopper optimisation algorithm: theory, variants, and applications. Ieee Access, 9, 50001-50024.

Zarei, A., Mousavi, S. F., EshaghiGordji, M., &Karami, H. (2019). Optimal reservoir operation using bat and particle swarm algorithm and game theory based on optimal water allocation among consumers. Water Resources Management, 33, 3071-3093.

Dhiman, G. (2021). SSC: A hybrid nature-inspired meta-heuristic optimisation algorithm for engineering applications. Knowledge-Based Systems, 222, 106926.

Bober, P., &Ferková, Ž. (2020). Comparison of an off-line optimised firing angle modulation and torque sharing functions for switched reluctance motor control. Energies, 13(10), 2435.

Cai, H., Wang, H., Li, M., Shen, S., Feng, Y., & Zheng, J. (2018). Torque ripple reduction for switched reluctance motor with optimised PWM control strategy. Energies, 11(11), 3215.

Dejamkhooy, A., & Ahmadpour, A. (2022). Torque Ripple Reduction of the Position Sensor-less Switched Reluctance Motors Applied in the Electrical Vehicles. Journal of Operation and Automation in Power Engineering.

Liu, L., Zhao, M., Yuan, X., & Ruan, Y. (2019). Direct instantaneous torque control system for switched reluctance motor in electric vehicles. The Journal of Engineering, 2019(16), 1847-1852.